Title

The N-glycome regulates the endothelial-to-hematopoietic transition

Journal

Science, 370(6521)

ISSN

0036-8075

Authors

Kasper, Dionna M

Hintzen, Jared

Wu, Yinyu

et al.

Publication Date

2020-12-04

DOI

10.1126/science.aaz2121

Peer reviewed

HHS Public Access

Author manuscript

Science. Author manuscript; available in PMC 2021 July 26.

Published in final edited form as:

Science. 2020 December 04; 370(6521): 1186–1191. doi:10.1126/science.aaz2121.

The N-glycome regulates the endothelial-to-hematopoietic transition

Dionna M. Kasper[1,2,3], **Jared Hintzen**[1,2,3], **Yinyu Wu**[1,2,3], **Joey J. Ghersi**[1,2,3], **Hanna K. Mandl**[1,2,3], **Kevin E. Salinas**[1,2,3], **William Armero**[1,2,3], **Zhiheng He**[1,2,3], **Ying Sheng**[4], **Yixuan Xie**[4], **Daniel W. Heindel**[5], **Eon Joo Park**[3,6], **William C. Sessa**[3,6], **Lara K. Mahal**[5,7], **Carlito Lebrilla**[4], **Karen K. Hirschi**[1,2,3,8,*], **Stefania Nicoli**[1,2,3,6,*]

[1]Yale Cardiovascular Research Center, Department of Internal Medicine, Section of Cardiology, Yale University School of Medicine, New Haven, CT 06511, USA.

[2]Department of Genetics, Yale University School of Medicine, New Haven, CT 06510, USA.

[3]Vascular Biology and Therapeutics Program, Yale University School of Medicine, New Haven, CT 06520, USA.

[4]Department of Chemistry, University of California, Davis, CA 95616, USA.

[5]Biomedical Chemistry Institute, Department of Chemistry, New York University, New York, NY 10003, USA.

[6]Department of Pharmacology, Yale University School of Medicine, New Haven, CT 06510, USA.

[7]Department of Chemistry, University of Alberta, Edmonton, AB T6G 2G2, Canada.

[8]Developmental Genomics Center, Cell Biology Department, University of Virginia School of Medicine, Charlottesville, VA 22908, USA.

Abstract

Definitive hematopoietic stem and progenitor cells (HSPCs) arise from the transdifferentiation of hemogenic endothelial cells (hemECs). The mechanisms of this endothelial-to-hematopoietic transition (EHT) are poorly understood. We show that microRNA-223 (miR-223)–mediated regulation of N-glycan biosynthesis in endothelial cells (ECs) regulates EHT. miR-223 is enriched in hemECs and in oligopotent nascent HSPCs. miR-223 restricts the EHT of lymphoid-myeloid lineages by suppressing the mannosyltransferase *alg2* and sialyltransferase *st3gal2*, two enzymes involved in protein N-glycosylation. ECs that lack miR-223 showed a decrease of high mannose versus sialylated sugars on N-glycoproteins such as the metalloprotease Adam10. EC-specific expression of an N-glycan Adam10 mutant or of the N-glycoenzymes phenocopied miR-223

* Corresponding author. stefania.nicoli@yale.edu (S.N.); kkh4yy@virginia.edu (K.K.H.).

Author contributions: D.M.K., J.H., and S.N. designed and conducted experiments, analyzed data, and wrote the manuscript. J.G., H.K.M., K.E.S., and W.A. carried out zebrafish experiments and analyzed data. K.K.H., Y.W., and Z.H. designed and performed mouse phenotypic experiments and analyses. C.L., Y.S., and Y. X. conducted glycomic and glycoproteomic analyses. L.K.M., D.W.H., W.C.S., and E.J.P. contributed N-glycome–related expertise and preliminary data. All authors edited the paper.

Competing interests: The authors declare no competing interests.

mutant defects. Thus, the N-glycome is an intrinsic regulator of EHT, serving as a key determinant of the hematopoietic fate.

In vertebrates, definitive hematopoietic stem and progenitor cells (HSPCs) are specified during embryogenesis by the transdifferentiation of endothelial cells (ECs) within the aorta-gonad-mesonephros (AGM) region of the dorsal aorta (1–3). This endothelial-to-hematopoietic transition (EHT) occurs in hemogenic ECs (hemECs), a subset of ECs that coexpress vascular and hematopoietic genes. The precise interplay between multiple signaling cascades (1, 2, 4) enables the progressive loss of endothelial and concomitant increase of hematopoietic gene expression, with hemECs giving rise to nascent HSPCs (2, 3). HSPCs then delaminate from the vascular wall and enter the circulation to colonize secondary hematopoietic organs, where they generate all blood cells throughout life (5–7). The EC and/or hemEC determinants that regulate EHT and thus HSPC production is not completely understood.

miR-223 is expressed in ECs undergoing EHT

Genetic deletion ofmicroRNA-223 (miR-223$^{\Delta/\Delta}$) results in excess nascent HSPCs in the zebrafish AGM (8). However, the mechanisms underlying miR-223 function in EHT are unknown (8–11). To examine miR-223 expression during EHT, we generated a zebrafish transgenic reporter in which miR-223–expressing ECs are labeled with both green fluorescent protein (GFP) and mCherry (miR-223:GFP^{+} kdrl: mCH^{+}) (Fig. 1A, fig. S1A, and materials and methods). EndogenousmiR-223 expression was enriched in miR-223:GFP^{+} kdrl:mCH^{+} cells versus miR-223:GFP^{-} kdrl:mCH^{-} cells (fig. S1B). Moreover, reexpression of miR-223 from its promoter inmiR-223:Gal4^{+} cells rescued the *cmyb*$^{+}$ HSPC overexpansion in miR-223$^{\Delta/\Delta}$ (fig. S1C). Thus, miR-223:GFP^{+} cells report the endogenous expression and function of miR-223.

miR-223:GFP^{+} kdrl:mCH^{+} cells were dispersed in a salt-and-pepper pattern, mostly within the AGM (Fig. 1A and fig. S1, D and E). The AGM population of miR-223:GFP^{+} kdrl:mCH^{+} cells increased from the onset to the peak of EHT, at 24 to 32 hours after fertilization (fig. S1E). They manifested a heterogeneous pattern of flat to bulging morphologies and underwent delamination from the AGM(Fig. 1A; fig. S1, F and G; and movie S1). miR-223:GFP^{+} kdrl:mCH^{+} cells showed elevated expression of endothelial (*kdrl*) and EHT markers, including *gata2b* and *runx1* in hemECs (12) and *cmyb* in nascent HSPCs (5) (fig. S1H). Accordingly, nascent HSPCs showed elevated expression of endogenous mature miR-223 (fig. S1I), suggesting that miR-223 is expressed in ECs undergoing EHT.

To further discern the distinct molecular subtypes among miR-223–expressing ECs, we performed single-cell RNA-sequencing (scRNA-seq) (fig. S2A and materials and methods). Kdrl:mCH^{+} ECs formed a vascular tree composed of branches that corresponded to embryonic specification trajectories, identified through the expression of known markers (fig. S2, A and B, and data file S1). We observed the arterial trajectory from which cells coexpress a continuum of early and late EHT markers in hemECs and in nascent HSPCs (Fig. 1B, fig. S2B, and data file S1). This branch split into two trajectories that included nascent HSPCs expressing early primed markers for the lymphoid-myeloid lineages or

lymphoid-erythroid lineages (Fig. 1C, fig. S2B, and data file S1). Gene ontology classifications of branch-defining genes confirmed that as ECs progressed through the EHT trajectories, they lost vascular development terms while gaining hematopoietic, protein biosynthesis, and N-glycosylation terms (13). Cell migration and cell cycle transcripts were mostly acquired within primed nascent HSPCs, when they likely begin to delaminate and/or amplify (fig. S2C and data file S2) (1, 2). Thus, our data suggest that oligopotent nascent HSPCs are produced during EHT in the AGM.

Additionally, we found that ECs that express *miR-223:gfp* transcripts comprised ~73 to 100% of hemEC-nascent HSPC and lymphoid-myeloid–primed HSPC branches and only ~17% of the lymphoid-erythroid–primed HSPC branch (Fig. 1D and fig. S2, D and E). *miR-223:gfp*$^{+}$ ECs had enriched expression of EHT, lymphoid-myeloid–, and lymphoid-erythroid– primed HSPC lineage markers in the relevant trajectories (fig. S2F and data file S1). Together, these analyses suggest that miR-223 is enriched in hemECs and nascent HSPCs during the EHT of oligopotent lymphoid-myeloid–primed HSPCs (Fig. 1E).

miR-223 limits hemEC and lymphoid-myeloid–HSPC production

To test miR-223 function in EHT, we phenotyped miR-223 mutants. Zebrafish miR-223$^{\Delta/\Delta}$ compared with wild-type embryos displayed an increase in gata2b:GFP^{+} or runx1:GFP^{+} hemECs in the AGM (Fig. 2A and fig. S3, A and B). As observed previously, cmyb:GFP^{+} kdrl:mCH^{+} nascent HSPCs were increased at 32 and 36 hours after fertilization in miR-223$^{\Delta/\Delta}$ (Fig. 2B) (8). Similarly in mice, miR-223 was abundantly expressed in ECs and hemECs from the embryonic day 10.5 (E10.5) AGM. Moreover, global removal of miR-223 (9) displayed elevated hemECs in the E10.5 AGM and HSPCs at secondary hematopoietic sites (fig. S3, C to F). These results suggest that miR-223 is a conserved inhibitor of hemEC and HSPC production.

Next, we determined whether nascent HSPCs in miR-223$^{\Delta/\Delta}$ zebrafish have altered behaviors. First, miR-223$^{\Delta/\Delta}$ versus control nascent HSPCs had increased proliferative capacity (fig. S4A). Second, delamination times from the AGM were significantly longer (2.3 ± 0.9 hours) for miR-223$^{\Delta/\Delta}$ as compared with wild-type nascent HSPCs (fig. S4B and movies S2 and S3). Although slowed, *cmyb*$^{+}$ HSPCs eventually delaminated and were still expanded in secondary hematopoietic organs of miR-223$^{\Delta/\Delta}$ embryos—namely, in the caudal hematopoietic tissue (CHT) at 2.5 days after fertilization (8), as well as in the thymus and kidney marrow at 6 days after fertilization (fig. S4C). Thus, the excess HSPCs in miR-223$^{\Delta/\Delta}$ exhibit aberrant proliferation and delamination.

Last, we examined how miR-223 loss affects blood lineage differentiation of the supernumerary HSPCs. Consistent with the relatively high expression of *miR-223:gfp* in lymphoid-myeloid–primed HSPCs in the AGM (Fig. 1D and fig. S2E), lymphoid and myeloid progenitors and differentiated cells were significantly expanded in secondary hematopoietic organs, whereas the erythroid lineage was unchanged (Fig. 2C and fig. S4D). Reexpression of wild-type miR-223 in miR-223$^{\Delta/\Delta}$ ECs normalized *cmyb*$^{+}$ HSPCs in the AGM and the lymphoid and myeloid blood cell lineages to control levels (Fig. 2, C and D,

and fig. S4E). These data suggest that miR-223 functions in ECs to restrict the EHT of lymphoid-myeloid–primed HSPCs.

miR-223 regulates N-glycosylation enzymes during EHT

miRNAs typically bind miRNA-responsive elements (MREs) within 3′ untranslated regions (3′UTRs) to fine-tune mRNA levels through decay and/or translational repression (14). Therefore, to identify miR-223 targets involved in EHT, we focused on transcripts that were up-regulated in miR-223$^{\Delta/\Delta}$ ECs and harbored a miR-223 MRE (8). We found that four out of the top eight candidate genes encode enzymes that regulate N-glycosylation (fig. S5, A to C, and data file S3).

N-glycosylation begins in the endoplasmic reticulum (ER), where a preassembled glycan core is attached onto specific asparagines (N) of nascent polypeptides. The glycan is progressively modified by glycosidases and glycosyltransferases as the protein traffics from the ER to the Golgi (fig. S5C) (15). The rate of glycan flux and/or the expression level of N-glycan biosynthesis enzymes (N-glycoenzymes) produce a diverse N-glycan repertoire, which determines protein activity and fundamental cell behaviors in reprogramming and oncogenesis (16, 17). However, N-glycosylation has not yet been implicated in EHT.

We investigated three canonical N-glycoenzymes that were derepressed in miR-223$^{\Delta/\Delta}$ ECs: *alg2*, an ER-resident mannosyltransferase that incorporates mannose moieties in the N-glycan core; *lman2lb*, a mannose-binding lectin that promotes N-glycoprotein transport from the ER to the Golgi; and *st3gal2*, a Golgi-resident sialyltransferase that terminally modifies N-glycoproteins with sialic acid sugars (fig. S5C and data file S3).

To determine whether miR-223 negatively regulates these N-glycoenzyme transcripts through their 3′UTRs, we constructed sensors consisting of mCherry fused to a 3′UTR fragment of *alg2*, *lman2lb*, or *st3gal2* that contains the putative miR-223 MRE (fig. S5D). The *alg2* and *st3gal2*.3′UTR sensors showed significant mCherry repression in the AGM of miR-223$^{\Delta/\Delta}$ versus control embryos. By contrast, the *lman2lb* 3′UTR sensor was similar between wild-type and mutant embryos (fig. S5D). These data suggest that miR-223 represses *alg2* and *st3gal2* transcripts through their 3′UTR in AGM ECs.

We next investigated how *alg2* or *st3gal2* repression contributes to miR-223–mediated regulation of EHT and HSPC production. We found that similar to miR-223, *alg2* and *st3gal2* were expressed in ECs and increased in nascent HSPCs at 27 hours after fertilization (fig. S6A). Morpholino-induced down-regulation of *alg2* or *st3gal2* expression reduced nascent HSPCs in the AGM, without otherwise affecting development (fig. S6, B to E). Moreover, partial down-regulation of *alg2* or *st3gal2*, which had no effect on wild-type embryos, rescued HSPC expansion in miR-223$^{\Delta/\Delta}$ embryos (fig. S6F). Congruently, *alg2* and *st3gal2* gain of function in ECs increased nascent HSPCs (fig. S7A). Likewise, mutation of the miR-223 MRE in the *alg2* or *st3gal2* 3′UTR (fig. S7, B to D) also recapitulated miR-223$^{\Delta/\Delta}$ phenotypes: hemECs and HSPCs were expanded in the AGM, as were HSPCs and differentiated lymphoid-myeloid lineage cells within the secondary hematopoietic

tissues (Fig. 3, A and B, and fig. S7, E and F). Together, these data suggest that miR-223 posttranscriptionally represses *alg2* or *st3gal2* to regulate EHT and HSPC differentiation.

The N-glycome controls EHT protein function

To test whether an altered N-glycome in ECs might lead to aberrant EHT in miR-223$^{\Delta/\Delta}$, we first profiled changes in specific glycan subtypes between wild-type and miR-223$^{\Delta/\Delta}$ ECs (Fig. 4A and fig. S8A). We found that high mannose (~71%) and sialylated complex/hybrid (C/H) (~18%) were the predominant glycans on proteins from wild-type ECs. By contrast, sialylated C/H (~97%) and sialofucosylated C/H (~3%) glycans were on proteins from ECs lacking miR-223, which was concomitant with a remarkable loss of high mannose type N-glycans (Fig. 4, B and C, and data file S4). Whole embryos overexpressing *alg2* or *st3gal2* in ECs or treated with the sialic acid precursor N-acetylmannosamine possessed both HSPC expansion and increased sialylated glycan subtypes at the expense of high mannose modifications, similar to those of miR-223$^{\Delta/\Delta}$ embryos (Fig. 4D; figs. S7A and S8, B to D; and data file S4). Thus, our analysis supports that the balance between high mannose versus sialic acid–containing N-glycan subtypes in ECs is regulated through miR-223–mediated repression of *alg2* or *st3gal2* N-glycoenzymes.

We next identified the N-glycoproteins that were altered in miR-223$^{\Delta/\Delta}$ compared with wild-type embryos (fig. S8E). The N-glycoproteins with reduced high mannose and/or increased sialylated C/H and sialofucosylated C/H modifications in miR-223$^{\Delta/\Delta}$ have known biological functions relevant to EHT and HSPC production, and their transcripts were expressed in ECs during EHT (Fig. 5A, fig. S8F, and data file S4). Of high interest was the metalloprotease Adam10a, which is critical for the proteolytic release of several cell surface proteins such as Notch, Vegfr2, tumor necrosis factor–α (TNF-α), and other EHT growth factor signaling molecules (18, 19). We found that the number of nascent HSPCs were significantly decreased in the AGM of *adam10a* guide RNA (gRNA)/Cas9–injected embryos, which is consistent with Adam10-mediated regulation of several EHT factors (Fig. 5, B and C, and fig. S8G). Down-regulation of *adam10a* in miR-223$^{\Delta/\Delta}$ decreased nascent HPSC numbers to wild-type levels, suggesting that Adam10a function was enhanced upon miR-223 loss (Fig. 5, B and C). We then over-expressed in ECs the wild-type *adam10a* or a N279 mutant version that prevents the high mannose attachment at this site (fig.S8,H and I) (20). We found that wild-type *adam10a*—and, even further, the *adam10a* N279mut—exhibited an expansion of nascent HSPCs in the zebrafish AGM (Fig. 5, B and C). These data suggest that decreased high mannose terminal modification of Adam10a promotes its function and contributes to the EHT phenotype of miR-223$^{\Delta/\Delta}$ embryos.

Discussion

Our study reveals a role for the N-glycan biosynthesis pathway in restricting the production of hemECs, HSPCs, and distinct blood lineages. We discovered an intrinsic mechanism that negatively regulates the transdifferentiation of ECs into oligopotent HSPCs on the basis of a “sugar code” comprising specific cell-surface glycans, high mannose, and sialylated C/H subtypes. This regulation is mediated through miR-223–dependent repression of N-glycan

biosynthesis genes, which controls the glycan repertoire to ensure normal HSPC production and differentiation (Fig. 5D and fig. S8J).

Loss of miR-223–mediated regulation of N-glycoenzymes causes a switch in N-glycans and enhances the function of N-glycoproteins. For example, Adam10a EC-autonomous activity is required for EHT but causes excessive HSPC production when lacking high mannose, probably through enhanced regulation of Notch, TNF-α, and/or other Adam10-dependent signaling pathways.

Furthermore, because EHT is a heterogeneous continuum of cell states (13), particular hemECs and nascent HSPCs could require miR-223 regulation of N-glycoprotein–dependent signaling to restrict EHT and balance blood production (Fig. 5D and fig. S8J). Congruently, N-glycoproteins throughout the EHT process could influence the differentiation of oligopotent HSPCs. Our findings lay the foundation for mechanistic studies of how protein N-glycosylation balances the diverse array of hematopoietic regulators during EHT.

The discovery that EHT is regulated by a specific glycan profile provides avenues to explore for the regulation of in vivo and ex vivo blood stem cell production (21). The wide variety of known glycan metabolism modifiers and inhibitors could be used to glyco-engineer hemECs, optimizing the production of glycoforms that facilitate somatic cell reprogramming to HSPCs (22). Thus, our findings could inform pharmacological strategies to produce HSPCs for therapeutic interventions.

Supplementary Material

Refer to Web version on PubMed Central for supplementary material.

ACKNOWLEDGMENTS

We thank M. Cavanaugh for fish husbandry and care and S. Mehta and the Yale Center for Genome Analysis for scRNA-seq bioinformatic analysis. We also thank A. Andersen (Life Science Editors), V. Greco, D. DiMaio, L. C. Boraas, and S. (Lily) Chen for critical reading of the manuscript. We apologize to those whose original work could not be cited because of space limitations.

Funding: This work was supported by grants from the NIH (F32HL132475, U54DK106857, and 1K99HL141687 to D.K.; R01HL130246 and R56DK118728 to S.N.; R01HL146056 and R01HL128064 to K.K.H; R01DK118728 to S.N. and K.K.H.; and R01GM049077 to C.L.) and the AHA (19PRE34380749 to Y.W. and 19TPA34890046 to S.N.).

Data and materials availability:

Bulk and single-cell RNA-seq data are submitted to the Gene Expression Omnibus (www.ncbi.nlm.nih.gov/geo/): GSE81341 and GSE135246. Raw Quant-seq reads are in the Sequence Read Archive (www.ncbi.nlm.nih.gov/sra): SRP099466.

REFERENCES AND NOTES

1. Clements WK, Traver D, Nat. Rev. Immunol. 13, 336–348 (2013). [PubMed: 23618830]
2. Gritz E, Hirschi KK, Cell. Mol. Life Sci. 73, 1547–1567 (2016). [PubMed: 26849156]
3. Jagannathan-Bogdan M, Zon LI, Development 140, 2463–2467 (2013). [PubMed: 23715539]
4. Kasper DM, Nicoli S, Curr. Stem Cell Rep. 4, 22–32 (2018). [PubMed: 29910999]

5. Bertrand JY et al., Nature 464, 108–111 (2010). [PubMed: 20154733]
6. Boisset JC et al., Nature 464, 116–120 (2010). [PubMed: 20154729]
7. Kissa K, Herbomel P, Nature 464, 112–115 (2010). [PubMed: 20154732]
8. Kasper DM et al., Dev. Cell 40, 552–565.e5 (2017). [PubMed: 28350988]
9. Johnnidis JB et al., Nature 451, 1125–1129 (2008). [PubMed: 18278031]
10. Trissal MC, DeMoya RA, Schmidt AP, Link DC, PLOS ONE 10, e0119304 (2015). [PubMed: 25793640]
11. Zhou W et al., Cell Rep. 22, 1810–1823 (2018). [PubMed: 29444433]
12. Butko E et al., Development 142, 1050–1061 (2015). [PubMed: 25758220]
13. Baron CS et al., Nat. Commun. 9, 2517 (2018). [PubMed: 29955049]
14. Bartel DP, Cell 173, 20–51 (2018). [PubMed: 29570994]
15. Moremen KW, Tiemeyer M, Nairn AV, Nat. Rev. Mol. Cell Biol. 13, 448–462 (2012). [PubMed: 22722607]
16. Lanctot PM, Gage FH, Varki AP, Curr. Opin. Chem. Biol. 11, 373–380 (2007). [PubMed: 17681848]
17. Pinho SS, Reis CA, Nat. Rev. Cancer 15, 540–555 (2015). [PubMed: 26289314]
18. van Tetering G et al., J. Biol. Chem. 284, 31018–31027 (2009). [PubMed: 19726682]
19. Hikita A et al., Biochem. Cell Biol. 87, 581–593 (2009). [PubMed: 19767822]
20. Escrevente C et al., Biochim. Biophys. Acta 1780, 905–913 (2008). [PubMed: 18381078]
21. Perlin JR, Robertson AL, Zon LI, J. Exp. Med. 214, 2817–2827 (2017). [PubMed: 28830909]
22. Boheler KR, Gundry RL, Stem Cells Transl. Med. 6, 131–138 (2017). [PubMed: 28170199]

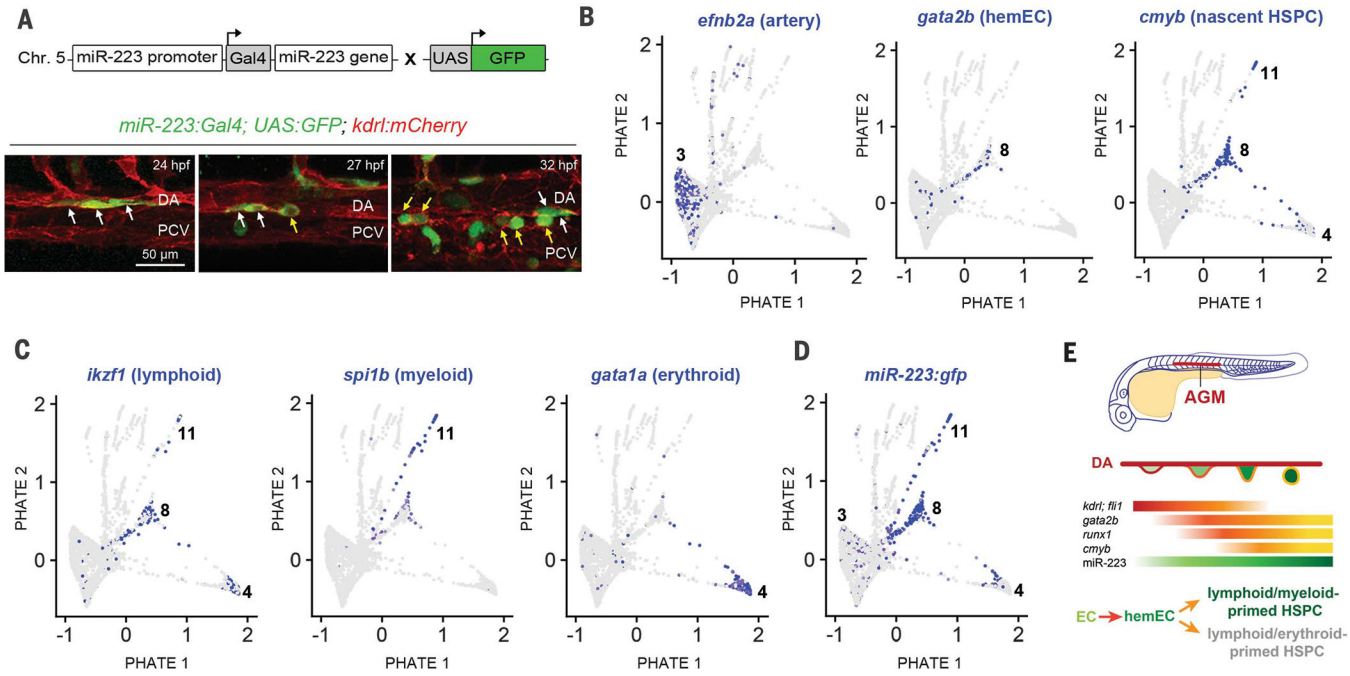

Fig. 1. miR-223 is expressed in hemECs undergoing EHT.

(A) (Top) Schematic of miR-223:GFP reporter. (Bottom) Lateral Z-projections of the zebrafish AGM. White and yellow arrows point to flat and budding miR-223:GFP$^+$ kdrl:mCH$^+$ cells, respectively. (**B** to **D**) Plots of wild-type kdrl:mCH$^+$ trunk ECs 27 hours after fertilization showing expression of (B) EHT, (C) blood lineage, and (D) *miR-223:gfp* genes (n = 6227 cells). Arterial (branch 3) and EHT (branches 8, 11, and 4) trajectories are indicated. (**E**) During EHT, a flattened EC (red outline) gains hemogenic potential (orange outline) and buds as a oligopotent nascent HSPC (yellow outline) from the DA wall. Gradients for endothelial and EHT markers are colored on the basis of their expression in the indicated cell types. The green gradient and text represent miR-223 expression. DA, dorsal aorta; hpf, hours post fertilization; PCV, posterior cardinal vein

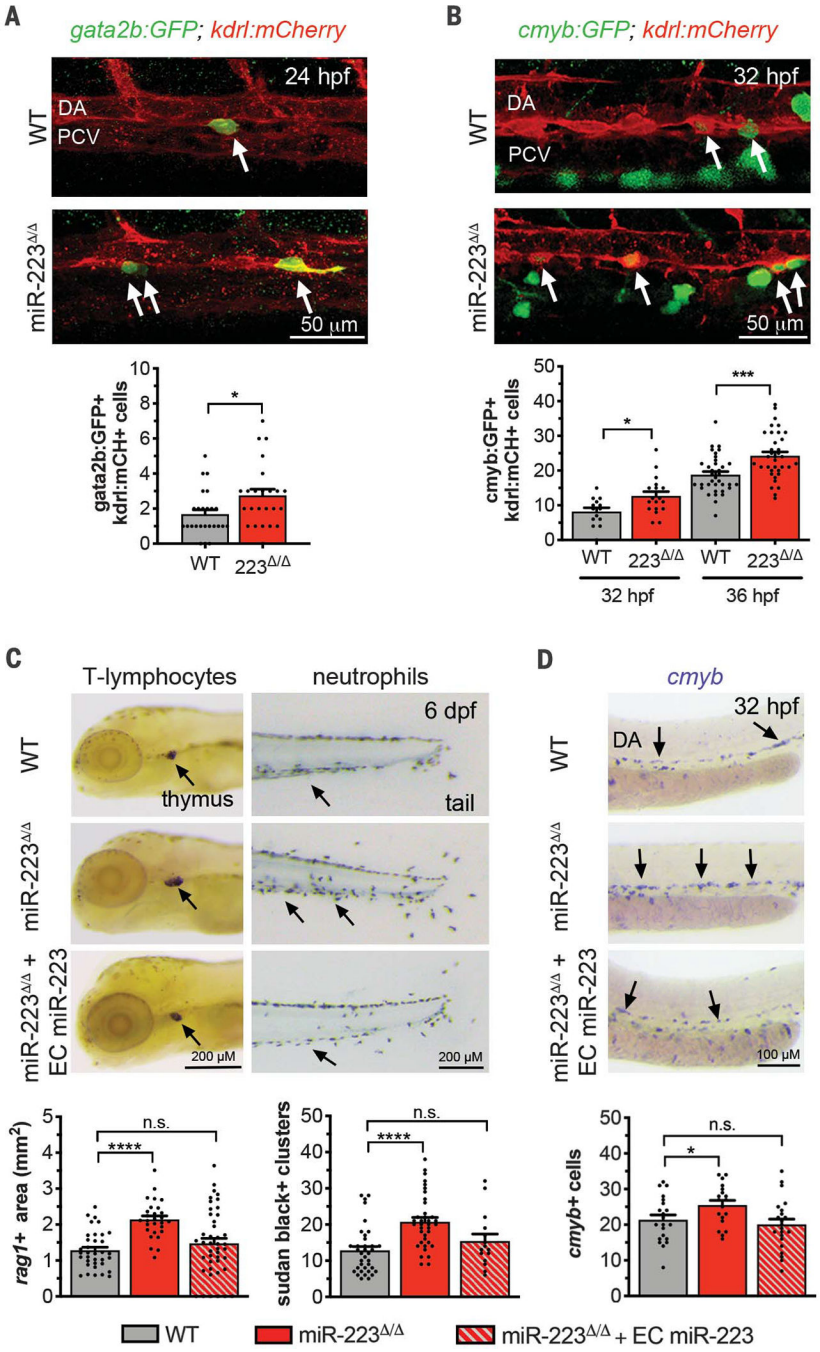

Fig. 2. miR-223 is an endothelial inhibitor of EHT and lymphoid-myeloid–oligopotent HSPC production.

(**A** and **B**) (Top) Z-projections or (bottom) mean ± SEM number of gata2b:GFP$^+$ kdrl:mCH$^+$ hemECs [n = 24 or 25 embryos, (A)] or cmyb:GFP$^+$ kdrl:mCH$^+$ nascent HSPCs [n = 13 to 18, 32 hours after fertilization; n= 34 to 36, 36 hours after fertilization (8), (B)]. (**C** and **D**) (Top) Representative images or (bottom) mean ± SEM area of (C) T-lymphocyte marker *rag1* expression (n = 18 to 35 embryos) and Sudan black$^+$ neutrophil clusters (n = 36 or 37 embryos) and (D) *cmyb* expression (n = 18 to 21 embryos). The EC miR-223 rescuing construct is described in fig. S4E. DA, dorsal aorta; dpf, days post fertilization; hpf, hours

post fertilization; PCV, posterior cardinal vein. Significance is represented as not significant (n.s.) $P > 0.05$, $*P \leq 0.05$, $**P \leq 0.01$, $***P \leq 0.01$, $****P \leq 0.0001$, unpaired, two-tailed Mann-Whitney U test.

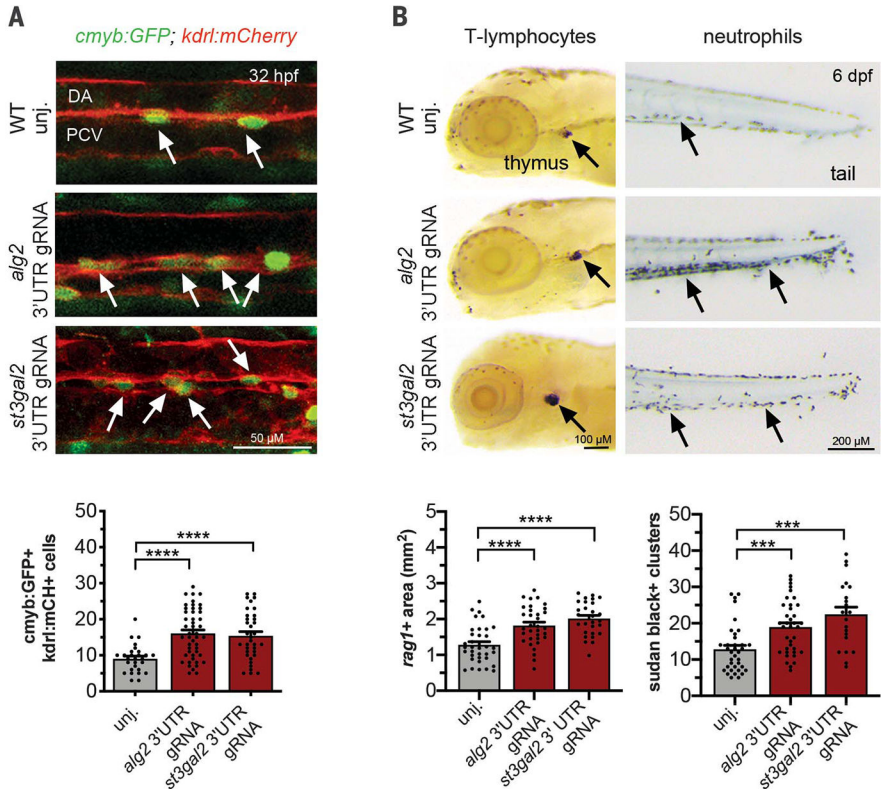

Fig. 3. miR-223 limits EHT and lymphoid-myeloid–oligopotent HSPC production through repression of *alg2* and *st3gal2*.

(**A**) (Top) Arrows indicate cmyb:GFP$^+$ kdrl:mCh$^+$ nascent HSPCs in the zebrafish AGM. (Bottom) Mean ± SEM of cmyb:GFP$^+$ kdrl:mCH$^+$ cells (n = 28 to 48 embryos). (**B**) (Top) Images or (bottom) mean ± SEM area of T-lymphocyte marker *rag1* expression (n = 28 to 35) embryos and Sudan black$^+$ neutrophil clusters (n = 21 or 37 embryos). Abbreviations and significance calculations are as in Fig. 2.

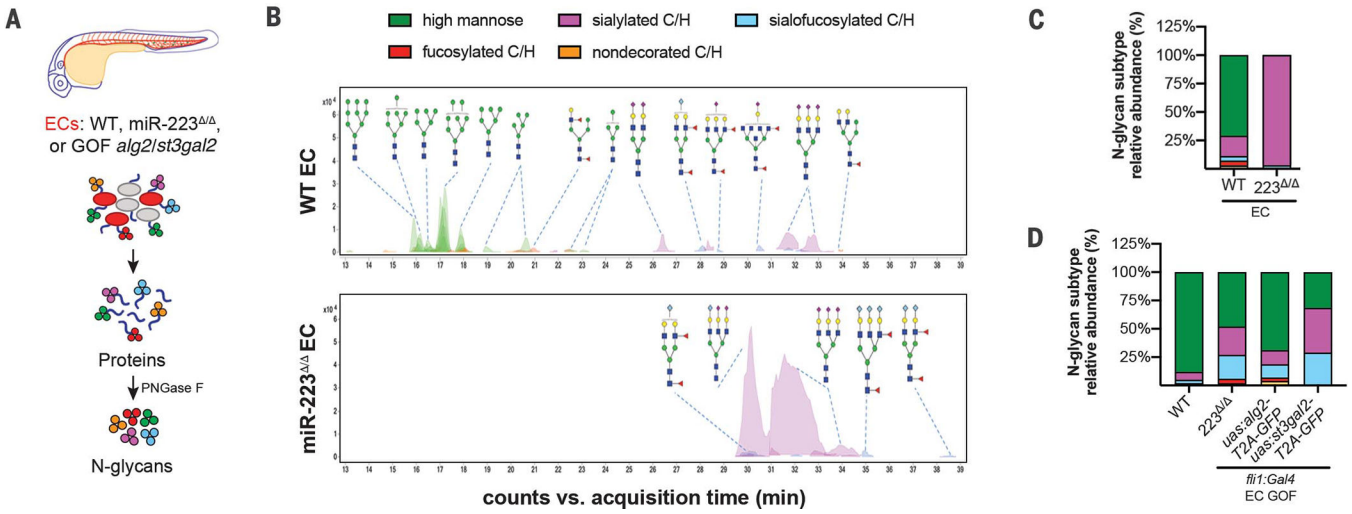

Fig. 4. miR-223 regulates the endothelial glycome.

(**A**) Extraction procedure to assess endothelial N-glycan profiles 27 hours after fertilization. Extracted N-glycans were analyzed by means of mass spectrometry (MS). (**B**) MS chromatograms for ECs showing relative abundance of N-glycan subtypes. A subset of the identified N-glycan structures are shown (monosaccharide legend is provided in fig. S8A). (**C** and **D**) Relative abundance of N-glycan subtypes in (C) ECs 27 hours after fertilization or (D) whole embryos. N-glycan subtypes are colored as in (B). EC GOF, endothelial cell gain of function.

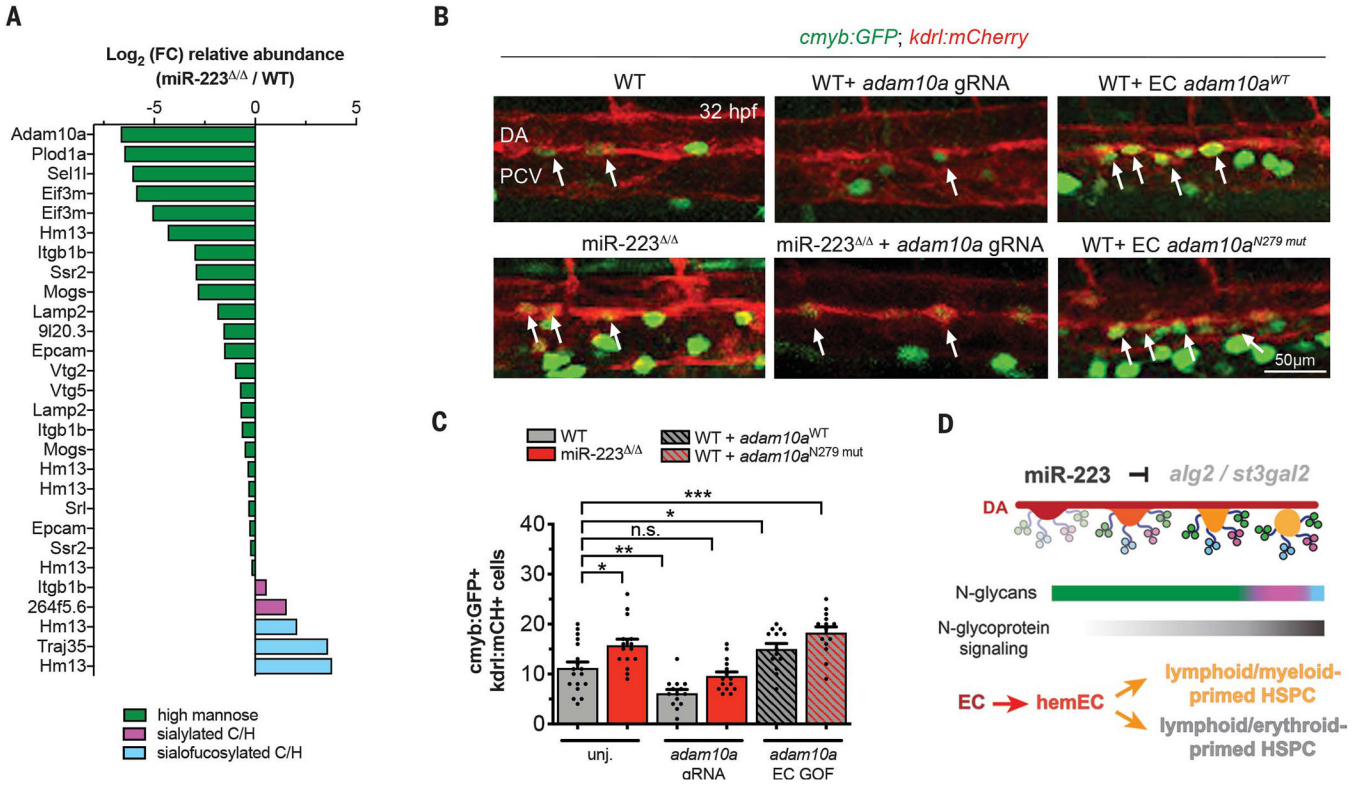

Fig. 5. A distinct N-glycan repertoire regulates protein function to limit EHT.

(**A**) Log_2 (fold change) of N-glycan relative abundance for miR-223–regulated N-glycopeptides (*n* = 3 replicates). (**B**) White arrows indicate nascent HSPCs in the zebrafish AGM of embryos injected with a gRNA that diminishes adam10a or with EC gain of function (GOF) *adam10a* constructs. (**C**) Mean ± SEM number of cmyb:GFP$^+$ kdrl:mCH$^+$ HSPCs (*n* = 13 to 18 embryos). Abbreviations and significance calculations are as in Fig. 2. (**D**) miR-223–dependent regulation of the N-glycome restricts EHT and lymphoid-myeloid HSPC production. In ECs, miR-223 represses *alg2* and *st3gal2* N-glycoenzymes, leading to high mannose-modified (green gradient) versus sialylated-modified (pink and blue gradients) proteins, which restricts (opacity) their signaling (black gradient). EHT cell types and N-glycan subtypes are colored according to Fig. 1E and Fig. 4B, respectively.